



**HAL**  
open science

## A 30 $\mu$ W Embedded Real Time Cetacean Smart Detector

Sebastián Marzetti, Valentin Gies, Paul Best, Valentin Barchasz, Sébastien Paris, Hervé Barthélémy, Hervé Glotin

► **To cite this version:**

Sebastián Marzetti, Valentin Gies, Paul Best, Valentin Barchasz, Sébastien Paris, et al.. A 30  $\mu$ W Embedded Real Time Cetacean Smart Detector. *Electronics*, 2021, 10 (7), pp.819. 10.3390/electronics10070819 . hal-03502818

**HAL Id: hal-03502818**

**<https://univ-tln.hal.science/hal-03502818>**

Submitted on 26 Dec 2021

**HAL** is a multi-disciplinary open access archive for the deposit and dissemination of scientific research documents, whether they are published or not. The documents may come from teaching and research institutions in France or abroad, or from public or private research centers.

L'archive ouverte pluridisciplinaire **HAL**, est destinée au dépôt et à la diffusion de documents scientifiques de niveau recherche, publiés ou non, émanant des établissements d'enseignement et de recherche français ou étrangers, des laboratoires publics ou privés.

Article

# A 30 $\mu$ W Embedded Real Time Cetacean Smart Detector

Sebastián Marzetti<sup>1,4</sup> , Valentin Gies<sup>1,2,4</sup> , Paul Best<sup>3,4</sup>, Valentin Barchasz<sup>1,2,4</sup> , Sébastien Paris<sup>3,4</sup>, Hervé Barthélémy<sup>1,4</sup>, Hervé Glotin<sup>2,3,4</sup> 

<sup>1</sup> Université de Toulon, Aix Marseille Univ, CNRS, IM2NP, Toulon, France

<sup>2</sup> Université de Toulon, SMIoT, Toulon, France - [www.smiot.fr](http://www.smiot.fr)

<sup>3</sup> Université de Toulon, Aix Marseille Univ, CNRS, LIS, DYNI, Toulon, France

<sup>4</sup> Université de Toulon, INPS, Toulon, France

\* Correspondence: [gies@univ-tln.fr](mailto:gies@univ-tln.fr); Tel.: +33 628357685

Version March 22, 2021 submitted to Electronics

**Abstract:** Cetacean monitoring is key to their protection. Understanding their behaviour relies on multi-channel and high sampling rate under-water acoustic recordings for identifying and tracking them in a passive way. However, a lot of energy and data storage is required, requiring frequent human maintenance operations. To cope with these constraints, an ultra-low power mixed signal always-on wake-up is proposed. Based on pulse pattern analysis, it can be used for triggering a multi-channel high performance recorder only when cetacean clicks are detected, thus increasing autonomy and saving storage space. This detector is implemented as a mixed architecture making the most of analog and digital primitives : this combination improves drastically power consumption by processing high frequency data using analog features and lower frequency ones in a digital way. Furthermore, a bioacoustic expert system is proposed for improving detection accuracy (in ultra low-power) via state-machines.

Power consumption of the system is lower than 30  $\mu$ W in always-on mode, allowing an autonomy of 2 years on a single CR2032 battery cell with a high detection accuracy. The receiver operating characteristic (ROC) curve obtained has an area under curve of 85% using expert rules and 75% without it. This implementation provides an excellent trade-off between detection accuracy and power consumption. Focused on sperm whales, it can be tuned to detect other species emitting pulse trains. This approach facilitates biodiversity studies, reducing maintenance operations and allowing the use of lighter, more compact and portable recording equipment, as large batteries are not longer required. Additionally, recording only useful data helps to reduce the dataset labelling time.

**Keywords:** Embedded Artificial Intelligence, Ultra-Low Power, Pattern Detection, Expert System, Biosonar, Always-On Wake-up, Pulse train.

## 1. Introduction

Every day, more than one hundred animal species disappear in the world. Since the 16<sup>th</sup> century at least 680 vertebrate species have been driven to extinction by human actions <sup>1</sup>.

Improving understanding of animals can help protecting them. Biodiversity monitoring is fundamental for that, using complementary techniques going from recorded video analysis to manual census. This article focuses on one of the most relevant technique : acoustic monitoring of animals emitting sound pulses, bursts or frequency chirps [1]. This category involves several species, from the

<sup>1</sup> <https://www.un.org/sustainabledevelopment/blog/2019/05/nature-decline-unprecedented-report/>

29 smallest such as insects or birds emitting trains of voiced pulses [2,3] to the largest mammals. Indeed,  
30 most of the biomass emits trains of pulses mainly for echolocation, sometimes with high frequency  
31 pulses, sometimes at lower frequencies. Biosonars are a perfect examples of trains of clicks or pulses  
32 emissions in different propagation environments: air for bats, water for marine mammals. While  
33 usually high frequency such as for bats, biosonars can also rely on low frequency voiced pulses trains:  
34 an example is the blue whale, emitting strong pulses at a frequency of 25 Hz.

35  
36 To illustrate our work, sperm whales (*Physeter macrocephalus*, Pm) have been chosen as a relevant  
37 case study. They use a biosonar to sense deep sea by echolocation, emitting click trains, and can be  
38 considered as a relevant case study as their echolocation technique is very close to other species. That  
39 means results obtained in this paper can be extended to other animals with minor adjustments such as  
40 modifying filters frequencies.

41  
42 Some cetacean species have been categorized as vulnerable among the endangered species. This  
43 is a result of anthropogenic activities creating chemical and acoustic pollution, leading to a slow  
44 decay of the populations. However, it is hard to cope with these global issues at a local scale. It is  
45 not the same with fishing or transportation activities [4] which also cause many cetacean deaths due  
46 to collision with boats or fishing by-catch [5,6]. In contrast with global issues, this can be locally  
47 avoided by detecting cetaceans in real time : some boat and whale collisions could be prevented if  
48 relevant alerts were sent to in time. This is the main purpose of this work, as well as monitoring them  
49 accurately in order to gather a better knowledge about them.

50  
51 Sperm whale monitoring is subject to several constraints. When installed in strict nature reserves,  
52 recording systems need to be autonomous for a very long time, leading to important requirements in  
53 battery life, especially if used in always-on mode. On the other hand, echolocation pulses contain high  
54 frequency information, requiring high sampling rate recordings, which consumes a lot of embedded  
55 energy. As these sea giants are rarely present, in standard always-on recorders, most of this energy  
56 is lost by recording empty sequences at a high sampling rate. In this sense, power consumption can  
57 be drastically reduced by activating high performance recording and analysis only when animals are  
58 suspected to be present. For our system, this relies on using an always-on ultra-low power wake-up  
59 detector as a first step. It is the topic of this paper. A case study on a real sperm whales data-set is  
60 presented with an embedded pulse detection technique. Detection accuracy is further improved by  
61 using an expert rules system to reject false positives.

### 62 1.1. Sperm whale biosonar

63 Sperm whales use echolocation for orientation and prey localization as shown in Fig. 1. Signals  
64 emitted are composed by sequences of clicks named *click trains*. [7–11]. A sperm whale click is a  
65 transient wave as shown Fig.2 and is composed of a direct and a reflected pulses emitted by pneumatic  
66 compression [12,13] (Fig.1). Depending on the relative orientation of the animal and the receiver, as  
67 well as the size of its head, the *Inter Pulse Intervals* (IPI) of this click going from 1 to 10 ms varies.  
68 Detection algorithms have to be compliant with these variations. IPI is an interesting feature to  
69 discriminate between species and will be discussed later in the paper, however in this study, as a proof  
70 of concept, we will first integrate ICI that is also a discriminant features of this species.

71  
72 Multipulsed clicks are transients (Fig.2) with a frequency spectrum going from 8kHz to 20kHz  
73 (Fig.3) [14–17]. Each click is separated from the next one by a time interval  $T_{InterClick} \in [100ms; 1s]$ .

74  
75 Cetaceans monitoring is complex because these mammals are spending most of their life in  
76 deep water, going down to 2000 m under sea-level and moving on long distances. Moreover, due  
77 to the sparsity of these animals, they are rarely present in a given area. Consequently, when an

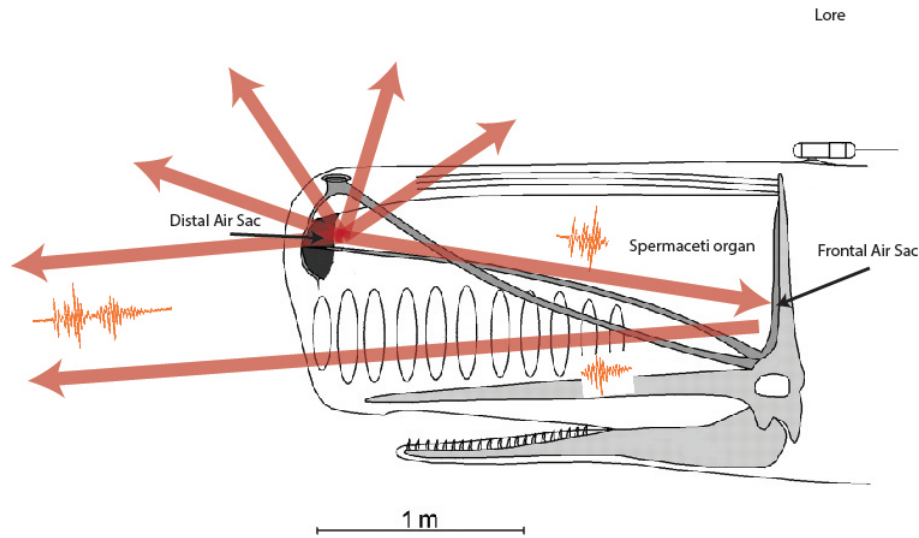


**Figure 1.** Sperm whale emission principle: a pulse is emitted by the distal air sac, propagated by the spermaceti organ and reflected by the frontal air sac.

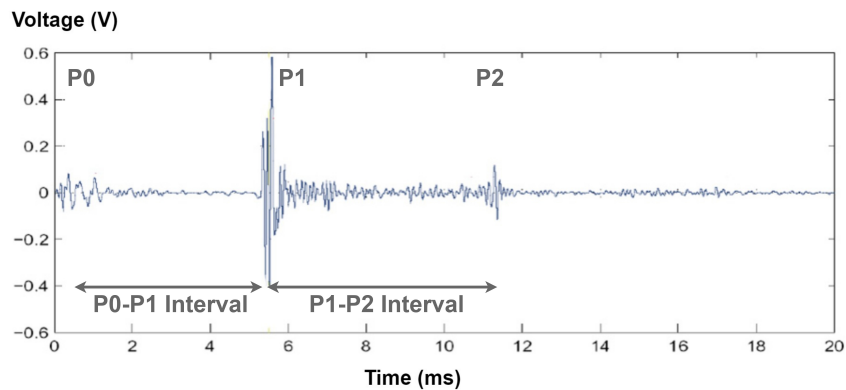


**Figure 2.** Physeter Macrocephalus click signal.

78 always-on recorder is used for monitoring, memory storage and energy are spent in an inefficient  
 79 manner. This is all the more crucial when high frequency recordings with multiple hydrophones  
 80 is performed (necessary to locate the acoustic emitters such as in [17–19]). This implies using large  
 81 batteries and storage capacities to be able to record in always-on mode sperm whales from multiple  
 82 hydrophones over a long period of time. This makes monitoring of these species a technical challenge,  
 83 as bio-environmental equipment is heavy, expensive, costly to install and maintain. Thus, reducing the  
 84 size and increasing autonomy of these recorders is key to facilitate biodiversity monitoring.

### 85 1.2. Keys to ultra-low power monitoring system

86 To achieve ultra low power consumption in monitoring systems, continuous recording is not an  
 87 efficient option as most of the time animals are not present. Instead, selective recording and analysis  
 88 of times an animal has been detected is preferable. We thus choose to keep only simple detectors  
 89 consuming a few  $\mu W$  always-on. In this way, power and data storage consumption can be drastically  
 90 reduced by recording data only when the probability of having a cetacean signal is high.

91

92 However, in order to achieve a state-of-art detection accuracy, using ultra-low power detectors  
 93 can be too limited. Instead of that, it is advisable to implement the detector in three stages as shown in  
 94 Fig.4 in green, orange and red. These three stages correspond to the three different types of embedded  
 95 artificial intelligence implementations, each one having a different magnitude of power consumption

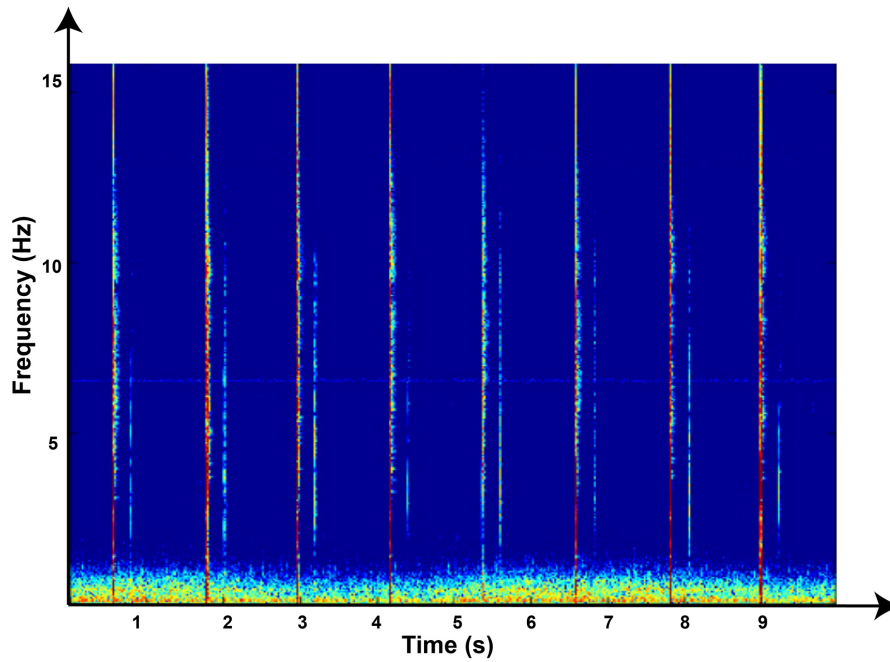


Figure 3. Spectrogram of a Sperm Whale click train.

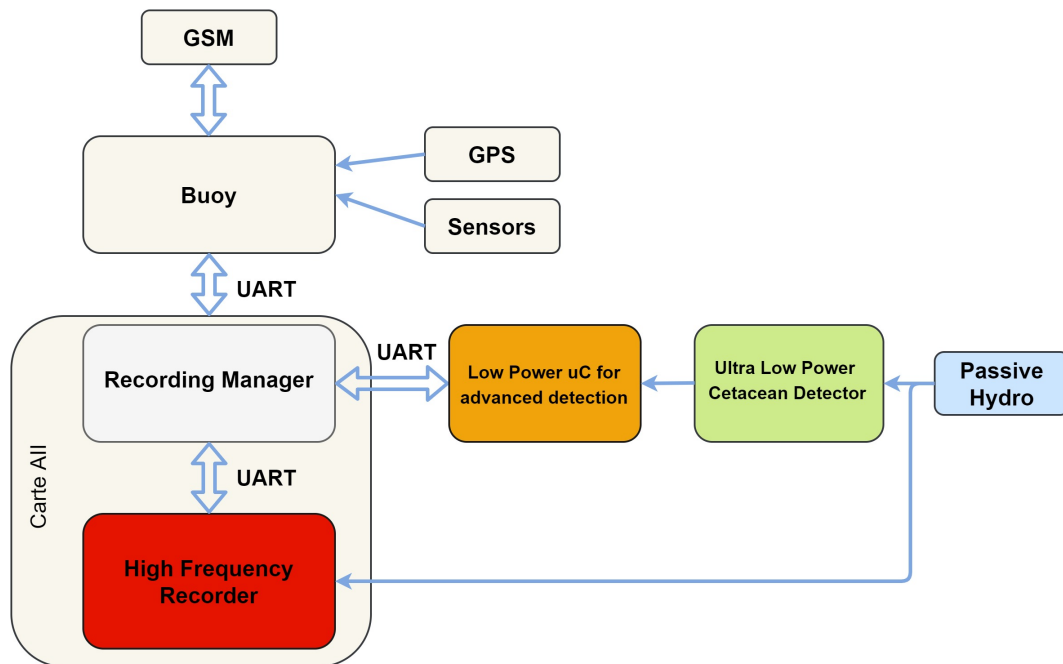
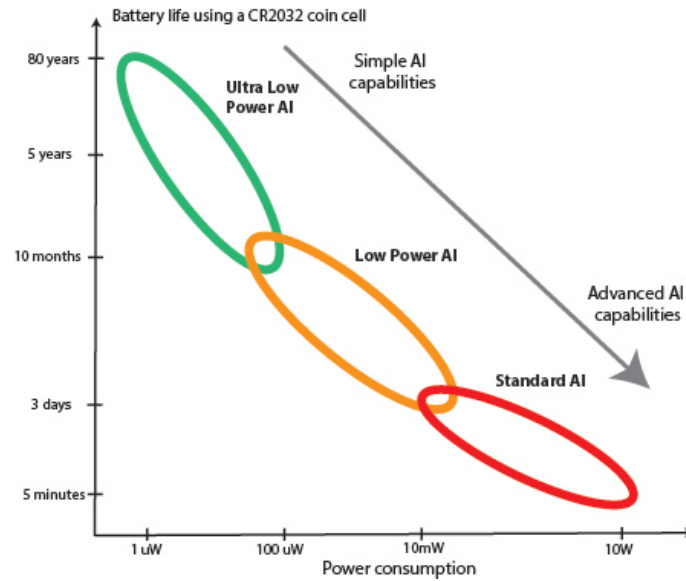


Figure 4. Cetacean Monitoring System.

96 as shown in Fig.5. These three stages are described here :

97

- 98
- 99
- 100
- 101
- 102
- 103
- First stage: an ultra-low power mixed signal analog-digital acoustic wake-up system (green block in Fig.4): It processes high frequency input signal using analog primitives, triggering an event when high energy pulses at specific frequencies occur. It is also robust to ambient sea noise, as the latter is measured using analog filters and a digital ultra low power processor working at low frequency. Having a power consumption of  $30 \mu W$ , it can be classified as an ultra-low power AI circuit as described in Fig.5.



**Figure 5.** Different types of embedded AI according to their power consumption

104 It also enters the category of ultra-low power wake-up, among other existing ones presented  
 105 in Tab. 1 and described here with their advantages and drawbacks. It is important to note that  
 106 in this comparison, most of proposed wake-up are standard envelope detectors without smart  
 107 features for improving their versatility and their detection capabilities such as :

- 108 – Adapting to ambient noise for adjusting detection level automatically.  
 109 – Classifying signals considering their spectrum.  
 110 – Implementing temporal pattern detection for improving classification based on expert rules.

Application	Frequency [Hz]	Ref	Power consump. [ $\mu W$ ]	Year	Noise immunity	Embedded AI
Seismic detection	$1.0 \times 10^2$	[20]	$4.0 \times 10^{-2}$	2015	No	No
Acoustic sensing and classification	$5.0 \times 10^2$	[21]	$1.2 \times 10^{-2}$	2018	No	Yes
Envelope detector wake-up	$1.0 \times 10^3$	[22]	1.8	2005	No	No
Voice activity detector wake-up	$5.0 \times 10^3$	[23]	6.0	2016	No	No
<b>Cetacean click detector</b>	$2.0 \times 10^4$	This paper	$3.0 \times 10^1$	<b>2021</b>	<b>Yes</b>	<b>Yes</b>
Ultrasonic envelope detector wake-up	$*4.1 \times 10^4$	[24]	1.0	2017	No	No
Ultrasonic wake-up	$*5.7 \times 10^4$	[25]	$8.0 \times 10^{-3}$	2019	No	No
Adjustable frequency detector wake-up	$3.0 \times 10^5$	[26]	$3.4 \times 10^1$	2018	No	No
AM signal detector wake-up	$3.2 \times 10^8$	[27]	7.4	2018	No	No
UHF signal detector wake-up	$2.0 \times 10^9$	[28]	$5.2 \times 10^1$	2008	No	No

\* Frequency cannot be changed

**Table 1.** Comparison of proposed cetacean click detector and existing wake-up.

111 This comparison is ordered by the frequency capability of the detector, considering this has a  
 112 strong impact on power consumption.

113 On of the most interesting implementation is a low frequency (500 Hz) acoustic signal processor  
 114 able to distinguish cars, trucks and generators noises for a power consumption equal to 12  $nW$   
 115 [21]. This one is too limited in frequency for cetaceans and cannot detect mixed temporal and  
 116 frequency patterns such as sperm whales clicks, but achieves a remarkable ultra-low power  
 117 consumption that can be considered as a milestone for a further silicon implementation of our  
 118 solution. Another wake-up detecting low seismic frequencies is proposed in [20], featuring a

119 very low 40 nW power consumption but without classification capabilities and with a limited  
120 frequency range (40 to 100 Hz). [22] is also an energy efficient (1.8  $\mu$ W) envelope detector working  
121 at 1kHz, but doesn't implement advanced AI features anymore. These first 3 implementations  
122 have a very low power consumption corresponding to limited operation frequencies, and cannot  
123 be used for cetacean detection because of that.

124 [24,25] are implementations able to deal with sperm whales signal frequencies. They are energy  
125 efficient but focused on detection of given and fixed specific ultra-sonic frequencies (41 kHz and  
126 57 kHz respectively). Used for remote activation of devices, they can not be used for pattern  
127 detection with temporal and frequency analysis. [26,29] have a wide input frequency range,  
128 but are based on digital or analog discrete circuits making their power consumption higher  
129 than previous implementations (34  $\mu$ W). However, they can be used for detecting an adjustable  
130 specific frequency in a narrow band, making them interesting for several applications, but cannot  
131 implement cetacean detection experts rules.

132 Higher frequency wake-up are proposed for comparison purpose such as [28] working at 2 GHz :  
133 it is a radio frequency (RF) detector having a power consumption of 52  $\mu$ W. [27] presents an  
134 interesting optimized envelope detector for amplitude-modulated (AM) signal at 315 MHz. It  
135 uses an interesting technique of frequency shifting using passive components for reducing power  
136 consumption, but can not implements AI detection rules.

137 Finally, none of the solutions presented in Tab.1 can be used for detecting cetaceans and more  
138 precisely sperm whales clicks : this is the topic of this paper and proposed solution is described  
139 extensively in Section 2, combining ultra-low power analog features and digital processing  
140 computed using the *sensor controller* of a low-power SoC. This allows to achieve low power  
141 detection of complex events based on their frequency and temporal attributes at a rather high  
142 frequency (20 kHz).

- 143  
144 • Second stage: a low-power micro-controller is implemented as a second stage detector (orange  
145 block in Fig.4), adding the ability to automatically tune the sensitivity of the first stage. It is  
146 implemented on a low power microcontroller (ARM M4). Described in Section 3.3, one of  
147 its features is a state machine implementing expert rules : events generated by the ultra low  
148 power detector (first stage) are analysed to avoid some false-positives and thus improving click  
149 detection reliability. Another option for this second stage could be to use an embedded shallow  
150 neural network such as in [30–32]. State machine analysis is performed only when events have  
151 been generated by the first stage, leading to a very low microcontroller activity (less than 0.01%  
152 of the time). Consequently, average power consumption of this stage is lower than the first  
153 one, even if this instantaneous consumption is a M4 microcontroller one during the analysis. A  
154 second state machine, is implemented to dynamically tune click detection sensitivity of the first  
155 stage detector, according to current false positive and true positive rates observed. It is described  
156 extensively in Section 2.
- 157  
158 • Third stage: a higher power 4-channels recorder (red block in Fig.4), able to compute  
159 deep-learning signal analysis, is triggered by the second stage. It allows recording several  
160 channels at a high sampling rate, but consumes a lot of energy (more than 1.2W). It implements  
161 24 bits analog digital converter (ADC), 512 *k*sps temporal resolution, and channel synchronization,  
162 all of which are key to allow sound source classification and localization. This recorder is started  
163 only when clicks have been validated by the expert rule state machine, reducing drastically its  
164 average power consumption compared to an always-on recorder. Active less than 0.05% of the  
165 time in real conditions (due to the sparsity of sperm-whales), it extends the battery life of the  
166 recorder by a factor 2000, reducing its average power consumption to less than 1mW. This allows  
167 an important battery and overall size reduction, easing its installation and maintenance while  
168 reducing its cost. This high resolution recorder named *Qualilife HighBlue* [18] has been designed

169 by SMIoT [33] but is not on the scope of this paper. It is used in Caribbean Marine Mammals  
170 Preservation Network (CARIMAM) project to monitor Caribbean underwater biodiversity at a  
171 large scale.

172

173 This data acquisition system is embedded in a waterproof sonobuoy designed by OSEAN company in  
174 France (Fig.6). This sonobuoy named Bombyx2, is the version 2 of Bombyx1 [34]. It is designed and  
175 used for the next five years to monitor cetaceans presence in real-time in order to prevent collisions  
176 with ships in Cetacean sanctuary Pelagos and elsewhere [5].

177



**Figure 6.** Bombyx2 - Project Interreg Maritime GIAS (whale anti-collision sonobuoy), here presented with communication antenna (4G or Iridium antenna) but without the acoustic 5 hydrophones antenna. The complete Bombyx2 is co-designed by LIS DYNI and IM2NP laboratories, SMIoT platform, OSEAN company.

178 It is important to note that this paper only focuses on the ultra-low power part of the wake-up  
179 system as well as the dynamic expert rules based tuning algorithm : Section 2 presents the ultra-low  
180 power cetacean click detector, Section 3 describes optimization of the algorithm using experts rules  
181 and automatic gain control. Results of both detector stages are discussed in their respective sections  
182 and a final conclusion is presented in section 4.

## 183 2. Ultra-Low Power Always-On Wake-Up Based on Acoustic Energy Analysis

### 184 2.1. System architecture

185 The ultra-low power sperm whales pulse detector first and second stage implementation is  
186 presented in Fig. 7 as a functional block diagram. It aims at detecting sudden increases in acoustic

187 level on well-defined frequencies (8 kHz to 20 kHz) characteristic of cetacean clicks. It relies on the  
 188 following circuits having ultra-low power consumption:

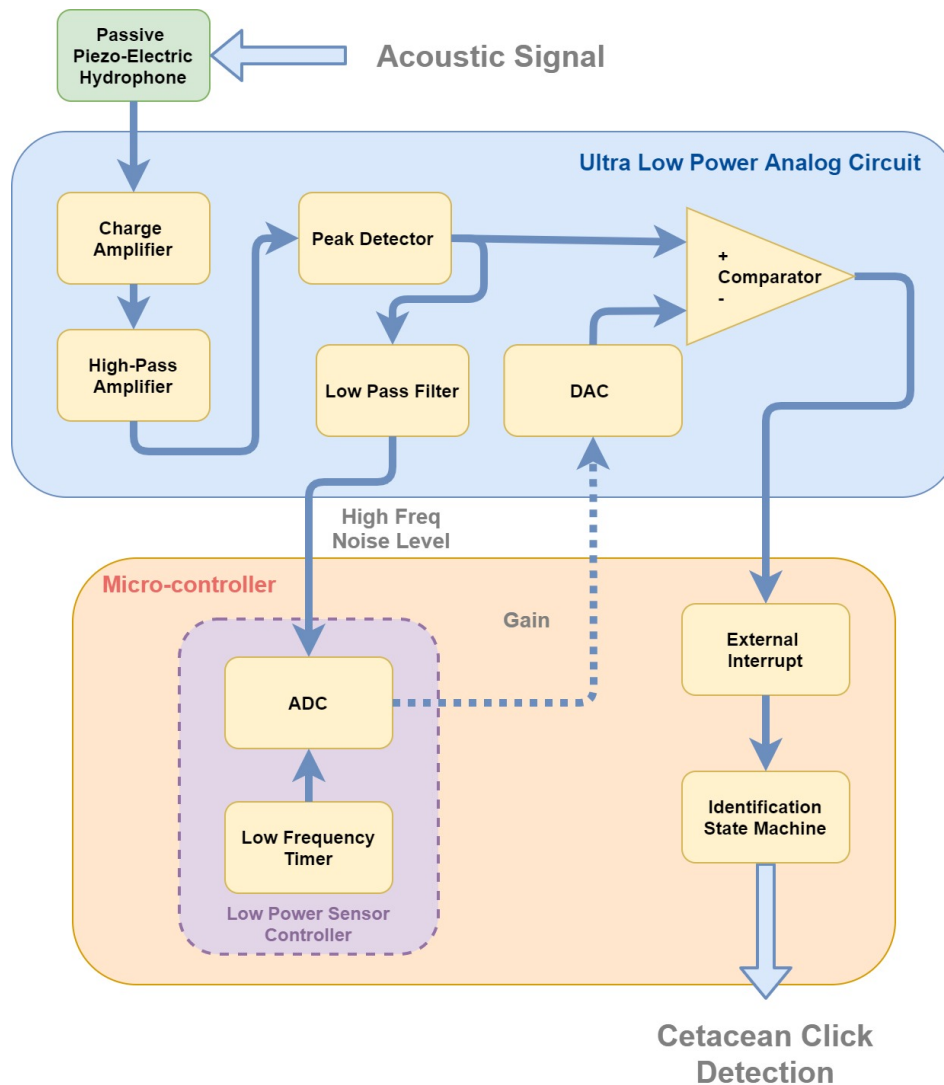


Figure 7. Sperm Whales detector block diagram.

- 189 • Passive piezoelectric hydrophone having a measurement bandwidth of 50kHz. This passive  
 190 sensor has been chosen to minimize power consumption, compared to amplified ones.  
 191
- Charge amplifier to amplify the piezoelectric charge signal. Integrator having a high input impedance, it converts acoustic piezo sensor charge into voltage, multiplying it by the inverse of the capacitance  $C_1$  in the feedback path as shown on Fig. 9. Without considering the additional resistor, this leads to:

$$V_{Out} = \frac{1}{C_1} \int \frac{dQ}{dt}$$

192 Additional resistor  $R_1$  forms a low-pass filter with  $C_1$  to limit the frequency bandwidth of  
 193 the hydrophone to 20 kHz, the maximum frequency present in sperm whales clicks. Power  
 194 consumption of this block is:  $0.9 \mu A$ .

- 195
- 196 • High-pass amplifier: as sperm whales pulse frequencies spread from 8 to 20 kHz, a band pass  
 197 filter is used to focus only on relevant signal. This filter gain Bode diagram is presented in Fig.

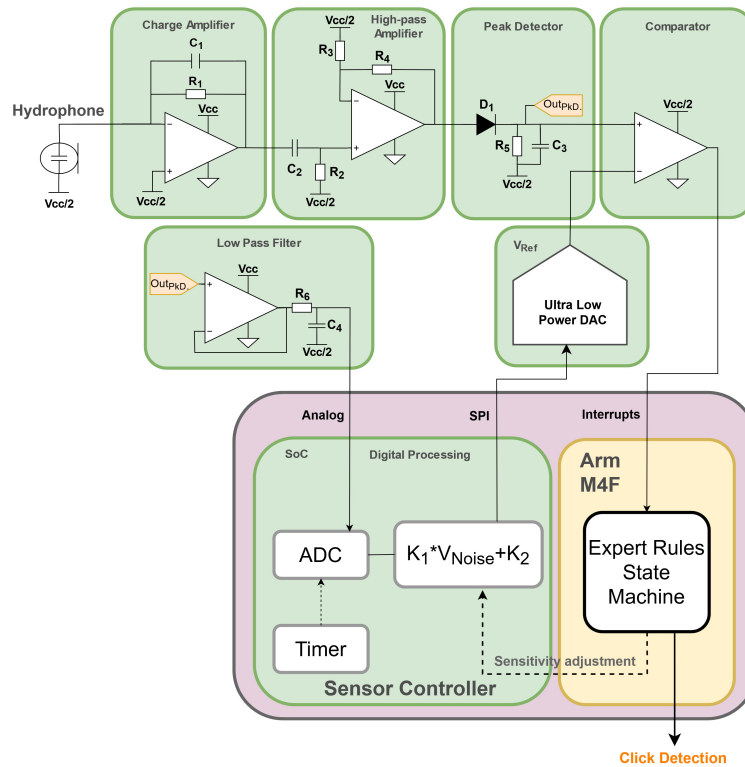


**Figure 8.** Electronic circuit of the always-on wake-up. ultra-low power parts are in green, low-power digital parts are in yellow. Voltage regulator and 1.65V reference are not presented.

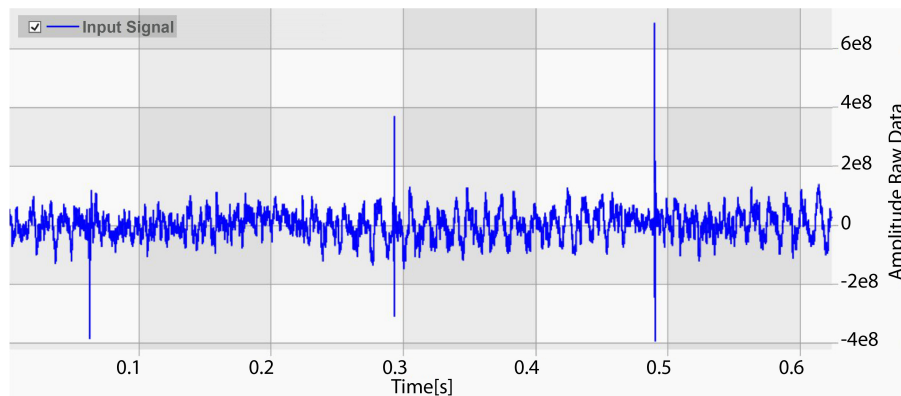


**Figure 9.** Cetacean click signal in output of the charge amplifier. Three clicks are present in the signal as well as sea noise.

198 10 . This band-pass filter is formed by the preceding low-pass filter and a high-pass amplifying  
 199 filter cutting near 8 kHz. Amplification factor is 10. An ultra-low power op-amp (MAXIM  
 200 MAX409A [35]) is used in this block, having a power consumption of  $1 \mu A$  for a gain bandwidth

product equal to 150 kHz, allowing amplification by a factor 10 at 15 kHz.

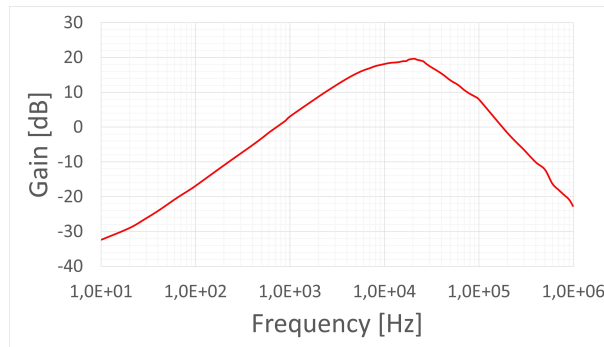


**Figure 10.** High-pass active filter measured frequency response.

- Low Pass Peak Detector: signal envelope is extracted using passive components: a diode [36] and a RC low pass filter having a time constant equal to 10ms. This peak detector gathers multiples click reverberations  $P0$ ,  $P1$  and  $P2$  (Fig. 2) of a cetacean click into one single detection as shown in Fig. 12. Power consumption of this passive block is null.

It is important to note that signal envelope is properly detected when input signal is increasing, but not when it is decreasing : output cannot decrease faster than the RC discharge. Thus, measuring output pulse time returns a result more related to pulse amplitude than to its duration. Improving this can be done by adding a reset circuit activated when input signal stays under a given threshold during a very short time. This have been considered in this work, but this circuit also add an additional power consumption that is not worthwhile. As explained in Section 3, it is useful to distinguish between cetacean clicks and periodic anthropogenic noise : sperm whales clicks are very short pulses (1 ms) separated by a long pulse interval (100 ms to 1 s) whereas common anthropogenic noises are mainly continuously repetitive ones (motor boats vibrations for example). In these conditions, adding a RC discharge having a duration of  $3RC = 30ms$  to the cetacean pulses doesn't affect the algorithm for detecting isolated pulses repeated with a long time interval. Thus, reset circuit is not necessary and has been removed.
- Low pass filter for sea noise estimation : in order to avoid false positives, average sea noise level must be estimated as a reference value for peak extraction. This is done using a low-pass filter with a cutoff frequency of 0.1 Hz in output of the peak detector. When a stationary noise is present, output  $V_{Noise}$  increases as it depends on the average of successive input signal amplitudes. In this way, a heavy swell or a motorboat cruising around the hydrophone will increase  $V_{Noise}$ , whereas an isolated sperm whale click will not change the input average amplitude and therefore  $V_{Noise}$ . Thus, this long period low-pass filter provides an estimate of the sea noise level in the frequency band of interest. To implement this block, a voltage follower (implemented using an operational amplifier LPV811 [37]) acting as a voltage buffer is added between the peak detector and the low-pass filter, consuming 600 nA.
- Comparator: this component is responsible for comparing the signal envelope (output of the peak detector) to a reference value  $V_{Ref}$  proportional to the estimated average sea noise level. When the output of peak detector block is higher than the reference value, a detection event is generated, triggering an interrupt in the processing microcontroller. The power consumption of this ultra-low power analog comparator is 320 nA.
- Reference value  $V_{Ref}$  generation: this feature is fundamental for the algorithm reliability. In a first approach, it seems evident to set  $V_{Ref} = KV_{Noise}$ . However, for a calm sea, this noise level will be very low, and possibly under the inner noise level of the hydrophone combined with its

amplifying chain, leading to an important false positive ratio detection. Thus, a constant has to be added to ensure a reliable detection. This leads to Equation 1 :

$$V_{Ref} = K_1 V_{Noise} + K_2, \quad (1)$$

where  $K_1$  and  $K_2$  are constants to be optimized according to AUC or specific functional points. Too small  $K_1$  and  $K_2$  generate false alarms as the reference level of the comparator is low, while high  $K_1$  and  $K_2$  constants result in a loss of smallest clicks of a distant sperm whale, as well as when the average sea noise level is important.

Doing these adjustments using analog circuits (Fig. 11) requires an adjustable constant generator, an adjustable amplifier and an adder. This solution has a power consumption of  $58 \mu A$ , mainly due to the use of digital potentiometers allowing up to  $1 M\Omega$  resistances, such as AD5222[38], consuming  $40 \mu A$ .

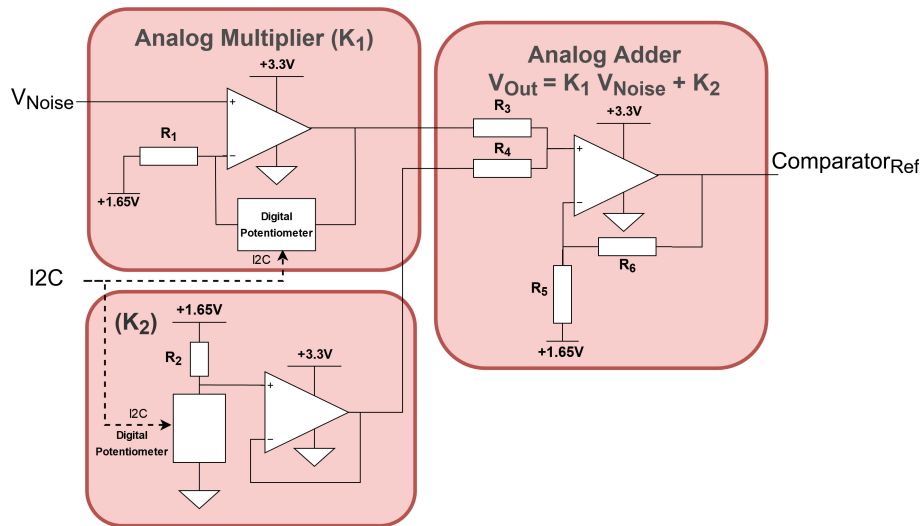


**Figure 11.** Alternative circuit diagram for comparator reference adjustment.

Compared with other parts of the analog front-end, the comparator reference adjustment power consumption is too high and needs to be reduced. There is another way of proceeding, less power consuming and more versatile : using an ultra-low power digital processor used to acquire average sea noise level  $V_{Noise}$  with an analog to digital converter (ADC) at a low sampling frequency rate. Then, computing  $V_{Ref}$  is done digitally and converted into an analog value entering the comparator, using an ultra-low power Digital Analog Converter (DAC). These operations are implemented using an ultra-low power system on chip (CC2652[39]) having a circuit dedicated to low frequency operations, named *sensor controller*. This circuit can be activated while the main processor is in sleep mode, leading to an ultra low power consumption of  $4 \mu A$  for ADC conversion of average sea noise level at 0.1 Hz. A LTC1662[40] DAC is used to convert the reference value transmitted by the *sensor controller* in SPI to an analogical value. Corresponding power consumption is  $1.5 \mu A$ , leading to an overall consumption of  $5.5 \mu A$ .

This shows that mixing analog and digital ultra low power techniques can be a power efficient way of processing an analog signal. It makes the most of using analog computations for high frequency signal processing and digital computations for low frequency ones.

It is important to note that in Equation 1, constants  $K_1$  and  $K_2$  are fixed hyper-parameters of the model that can be adjusted by grid search algorithms in order to maximize click

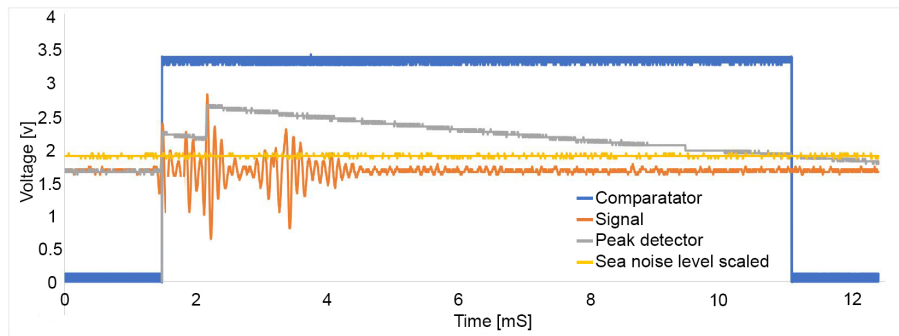


**Figure 12.** Real cetacean clicks and analog detection algorithm waveforms. High-pass filtered input signal is in orange,  $V_{Ref}$  in yellow, click envelope in grey and comparator output in blue.

detection accuracy as described in 2.2. However, depending on experimental conditions such as anthropogenic noise, sea noise evaluation can be biased, leading to false alarms. In this case, algorithm reliability can be improved by adjusting dynamically  $K_1$  and  $K_2$  in order to avoid false alarms. This adjustments are done using a state machine based automatic gain control introduced in Section 3.

- Voltage regulator: a 3.3V supply voltage value has been chosen. Powered by a single Li-Ion 3.7V cell, a Microchip MCP1810[41] linear voltage regulator is used, having a power consumption of 20nA. Reducing the input voltage to 1.8V would be a good option and will be done in a further work.
- Voltage reference: a single 3.3V supply is used, requiring to generate a virtual 1.65V ground voltage. This is done using a 1.65V voltage divider followed by an analog buffer (using a LPV811 operational amplifier[37]) having a current consumption of 0.58  $\mu A$ .

Table 2 shows the power consumption of each circuit used in the ultra-low power part of the click detector, leading to an aggregated power consumption of 12.5  $\mu A$ , without using expert system state machines. Measurements have been done using a custom mixed analog-digital breadboard shown on Fig. 13 and designed for this project. This board is fully functional and allows to measure precisely power consumption of each analog and digital modules by physically connecting or disconnecting power supplies of each stage. Considering there are limited space constraints in the sonobuoy, this breadboard has been used in this form during experiments. Its size will be reduced in the future, but without changing anything to the implemented analog features. However, it is noticeable that many available features in the development board shown on Fig 13 have not been used. 4 Sallen-Key structures, 4 multiple feedback (MFB) structure, 4 peak detectors, 2 DAC, 4 passive filters, 4 comparators and 4 delay lines are available on the board, with a CC2652 for the digital part. Only 2 Sallen-Key structures, 1 peak detector, 1 passive low-pass filter, 1 comparator and the CC2652 SoC have been used for implementing the system (plus one more analog structure for the charge amplifier that can be implemented using an additional MFB structure, but is not in the scope of this paper). Each block of the analog implementation is detailed in Table 2.

## 2.2. Results

Signal waveforms obtained using the analog detection algorithm are shown on Fig. 12. As explained before, an important feature of the proposed ultra-low power cetacean detector is the ability to automatically tune the comparator reference value  $V_{Ref}$  described in Eq. 1 depending on the sea ambient noise. This equation uses 2 fixed hyper-parameters  $K_1$  and  $K_2$  that have to be optimised in

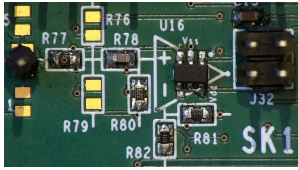
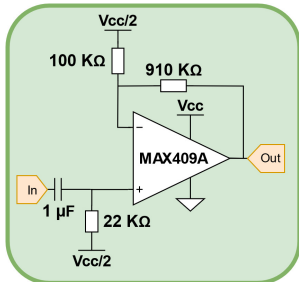
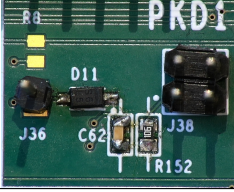
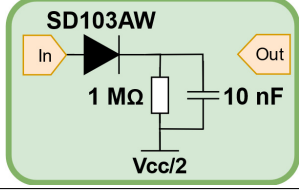
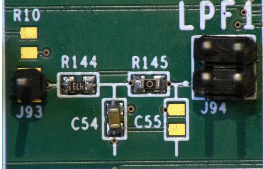
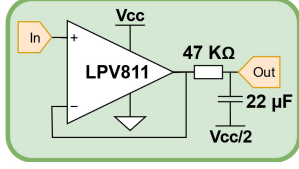
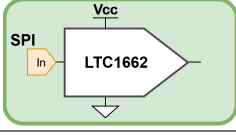
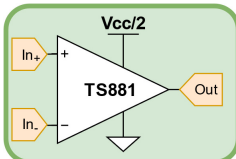
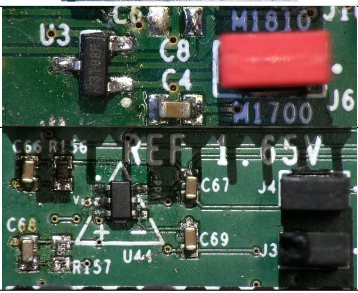
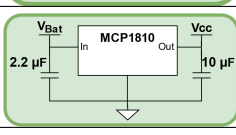
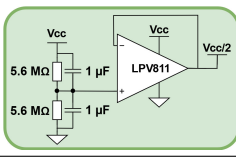
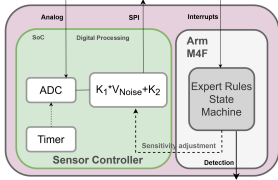
Circuit	Current [ $\mu A$ ]	Picture Board	Schematic	Associated datasheet
High-pass Amplifier	4.0			MAX409 [35]
Peak Detector	–			SD103AW [36]
Sea noise Low frequency Low-pass Filter	0.6			LPV811 [37]
DAC	1.5			LTC1662 [40]
Comparator	0.3			TS881 [42]
voltage regulator	0.02			MCP1810 [41]
1.65V voltage reference	0.58			LPV811 [37]
Sensor Controller using a 10 Hz timer	4.5			CC2652 [39]
Complete ultra-low power hardware	12.5			

Table 2. Always-on ultra-low power analog circuits implementation and power consumption ( $\mu A$ ).

298 order to maximise classification accuracy.

299

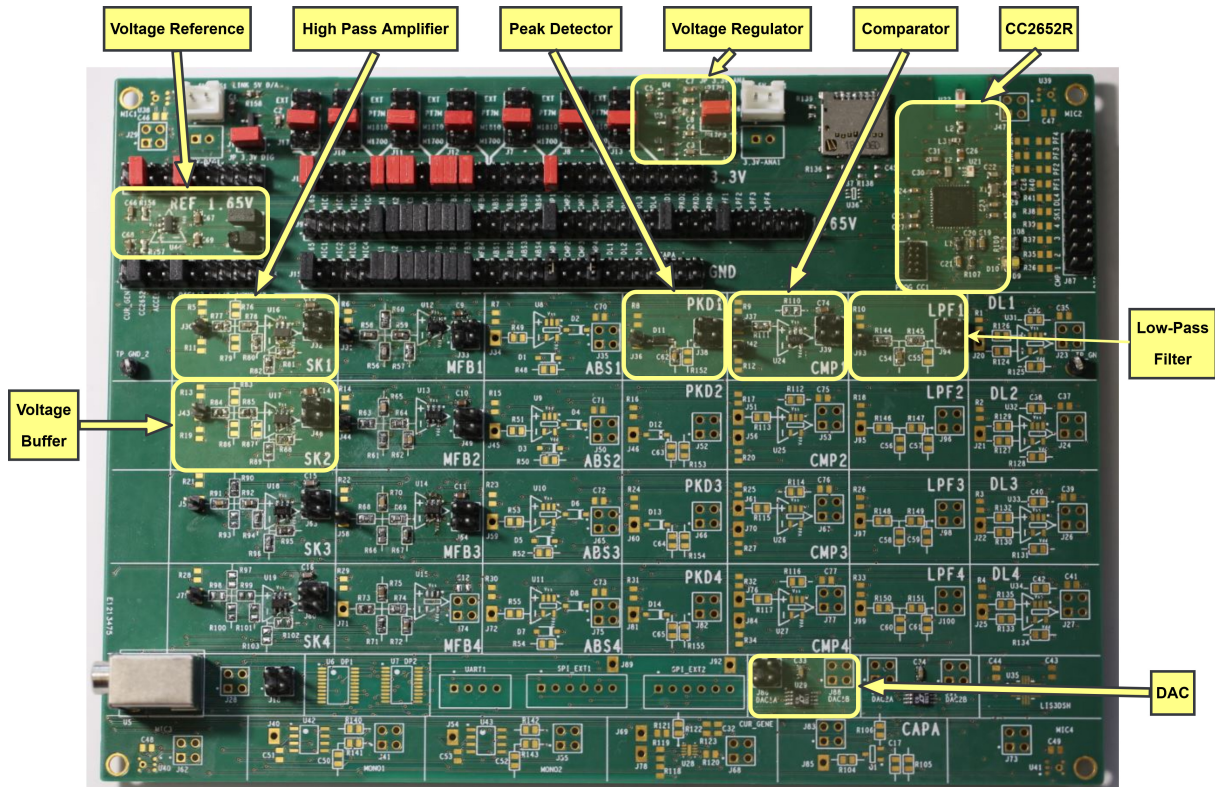


Figure 13. Analog test and power measurement board.

300 Performance is evaluated using a test set of 100 underwater recordings, with and without sperm  
 301 whale clicks. They are chosen at random in a labelled database composed of samples from the  
 302 BOMBYX project sonobuoy [34]. The dataset is composed of 8% of clean samples, and 92% of noisy  
 303 ones (either boat noise or white noise were added at  $-6, 0, 6, 12, 18, 24$  dB signal-to-noise ratio (SNR)).  
 304 There is equal number of positive and negative samples. For *Findability, Accessibility, Interoperability,*  
 305 *and Reuse* (FAIR) comparisons to other detectors, the full labeled dataset (including pulses of another  
 306 mediterranean fin whales) is available online at [SABIOD.org](http://SABIOD.org)<sup>2</sup>.

307

308 Receiver Operating Characteristic (ROC) curve of the ultra-low power click detector is presented  
 309 in blue in Fig. 15: Area Under the Curve (AUC) is 75%. An optimal configuration corresponds to  
 310  $K_1 = 4.3$  and  $K_2 = 0.25V$ . This is a relevant achievement considering system power consumption is  
 311 only  $12.5 \mu A$ . Moreover, it is important to note that the reference database is mainly focused on sperm  
 312 whales and motorboats but has very few samples of silent sea. Consequently, detecting clicks on this  
 313 database is much more difficult than it would be in real conditions with a frequently quiet sea.

### 314 3. Improving click detection using expert bioacoustic rules

315 The proposed ultra-low power click detector relies on the real time analysis of the input acoustic  
 316 signal in order to detect a sudden increase in its energy. The output of the comparator corresponds to a  
 317 logical 1 during a click. However, other types of acoustic signal having a high level in high frequencies,  
 318 such as a motorboat running close to the hydrophone, can also trigger the comparator, leading to false  
 319 alarms.

<sup>2</sup> <http://sabiod.org/pub/dataset/PhyseterM-and-BalaenopteraP-dataset.zip>

### 3.1. Implementing expert rules in ultra-low power using state machines

In order to improve the accuracy of the detection algorithm, an ultra-low power improvement based on two bioacoustical expert rules is proposed. It relies on :

- Click duration : a cetacean click has a well-known shape [13], its main peak lasts between  $50 \mu\text{s}$  and  $200 \mu\text{s}$  and can be repeated a few times. This first expert rule is used to decide whether the received pulse fits this interval or not, corresponding to a high probability for the received signal to be a click.
- Inter-click interval : time between two successive clicks is also well-defined ( $Interval \in [100\text{ms}; 1\text{s}]$ ) [13] and can be used as a second expert rule to confirm if two successive clicks can be part of a click train or not. Process is iterated on each new click.

These expert rules can be implemented efficiently using a micro-controller. As described in the left diagram of Fig.14, it relies on a simple state machine, leading to a very low additional power consumption. When an event (rising edge) is generated in output of the comparator, meaning that a high energy signal has been received in the given frequency band, the state machine starts waiting for a falling edge. The latter corresponds to the end of the high energy pulse whose duration is compared to a reference interval (the first expert rule) in order to determine whether the pulse is consistent with the possible acoustic emission of sperm whales or not. If it is, a click counter is incremented and the next click detection is started. If the click is not the first one, inter-click duration is calculated and compared to a second reference interval using the second expert rule. If the inter-click duration is in the interval, click detection is validated and a *true positive* (TP) counter is incremented, otherwise a *false positive* (FP) counter is incremented.

### 3.2. Automatic gain control

As described before, using expert rules also allows to get indications on the number of true and false positives. This is useful to fine tune the main detection algorithm and especially  $K_1$  and  $K_2$  constants used to generate the comparator reference as described in Equation 1. If the constant is too high, clicks will be missed, if it is too low, the comparator output will be triggered on unwanted signals. In order to dynamically adjust these constants, a second state machine implementing an automatic gain control has been proposed and is shown on the right side of Fig. 14. It uses the false-positive and true-positive counters incremented in the click detector state machine. Each time a click is identified as part of a click train, the true positive counter  $Count_{TP}$  is incremented. Each time a pulse or an inter-pulse length does not comply with the expert rules, the false positive counter  $Count_{FP}$  is incremented. Periodically, these counters values are reset to 0. Following situations can occur as shown in the state machine of Fig.14 :

- If  $Count_{FP} = 0$  and  $Count_{TP} > 0$ , clicks are detected. In this situation, gain is well-tuned and is not adjusted.
- If  $Count_{FP} = Count_{TP} = 0$ , nothing is detected, neither clicks nor other signals. Sensitivity of detection can be increased by reducing simultaneously gain  $K_1$  and  $K_2$ , with a minimum value of  $K_1 = 2$ . This reduces the reference voltage corresponding to the sea noise level (yellow line on Fig.12)
- If  $Count_{FP} > 0$ , false alarms are present, and gains  $K_1$  and  $K_2$  have to be increased simultaneously in order to avoid detection of sea noise. This can happen when weather conditions are changing very quickly or boats are approaching.

Considering power consumption, this automatic gain control can be implemented in ultra-low power, because adjustment is done when a click has been validated or not in a few  $\mu\text{s}$ .

### 3.3. Results

Results (ROC curves) of the improved detection algorithm using expert rules are shown on Fig.15. Performance is evaluated using the same test set of 100 recordings as for the click detection algorithm.

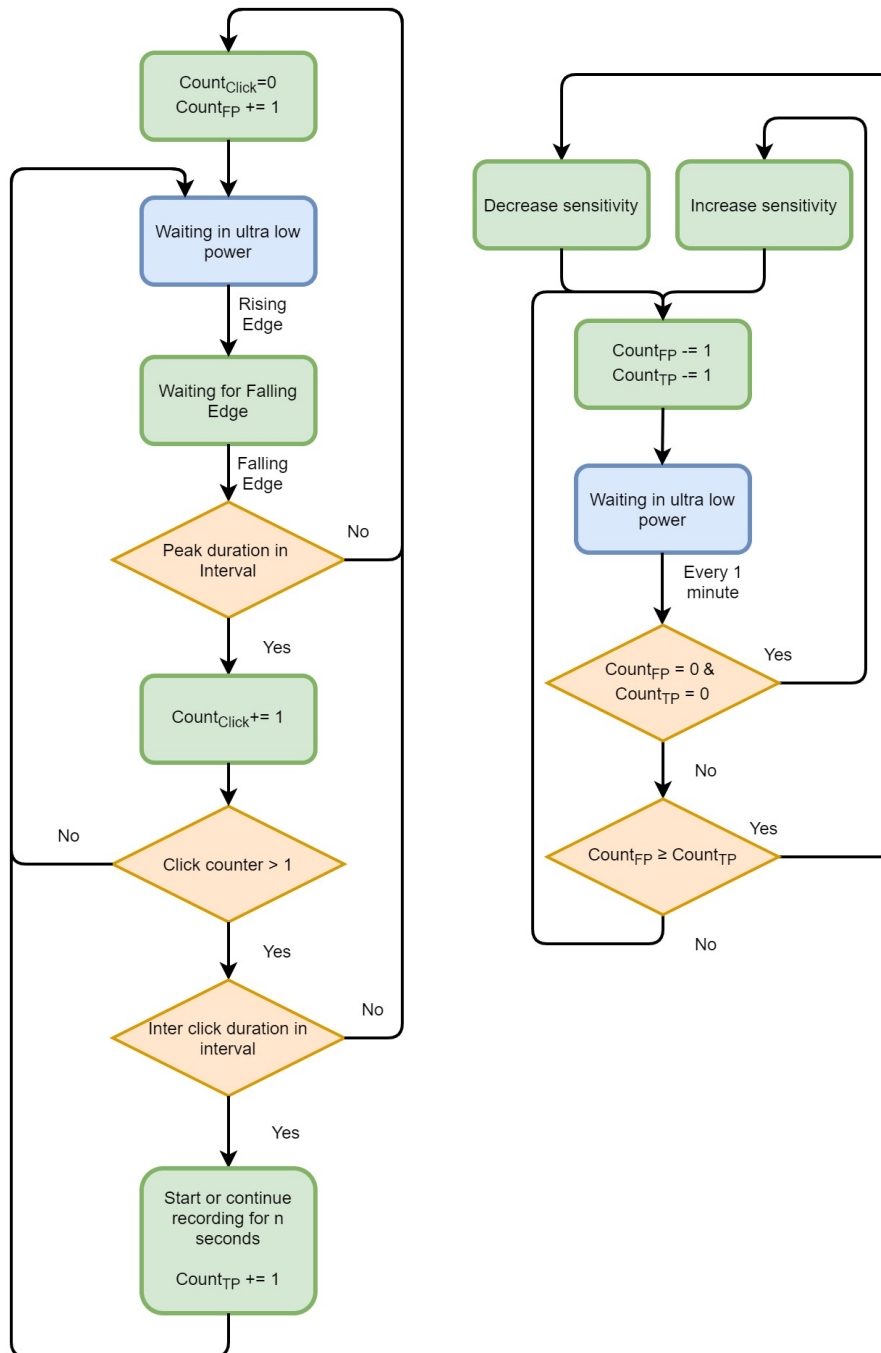


**Figure 14.** Cetacean click detection state machine (left), and automatic gain control state machine (right).

367 Area Under the Curve (AUC) is equal to 85%, compared to 75% without using the expert rules.

368

369 Power consumption impact of these expert rules and automatic gain control is low: current  
 370 is increased by  $4.5 \mu A$  (measured value), mainly because of a timer used for evaluating pulse and  
 371 inter-pulses duration has been activated. This limited additional power consumption allows to avoid  
 372 false alarms, reducing the number of high frequency recorder activation, thus saving battery power by  
 373 avoiding unnecessary high-power recordings.

374

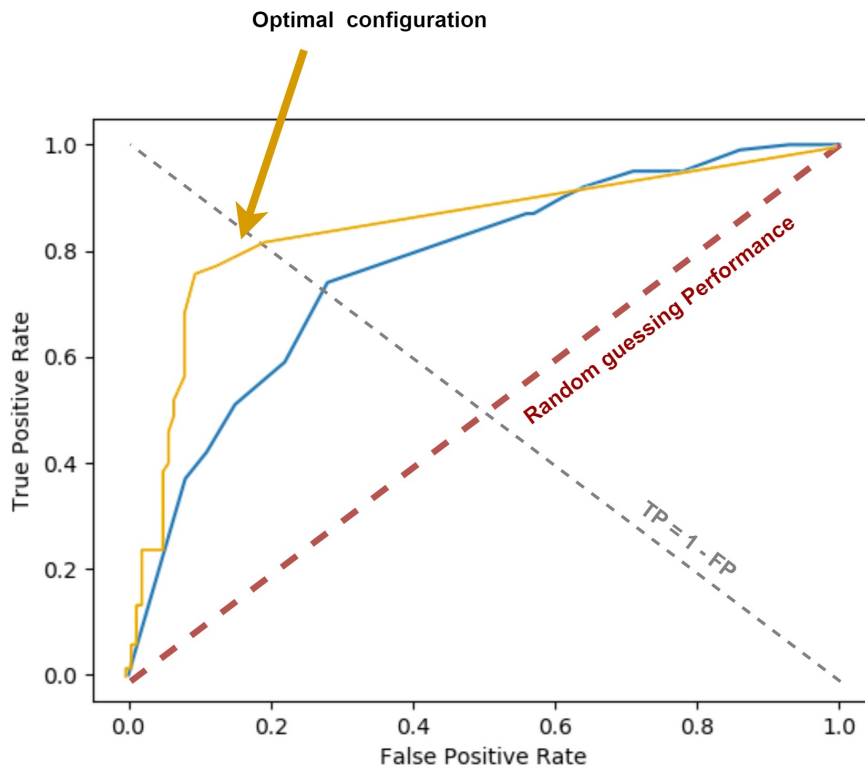


**Figure 15.** Click detector ROC curve using the state machine and expert rules validation (in yellow), versus without it (in blue) for different values of  $K_1$  parameter. Area under the ROC curve is 85% using the state machine and expert rules, versus 75% without.

375 Proposed embedded ultra-low power cetacean detector can also be compared with a standard  
 376 solution using a convolutional neural network (CNN) [43], trained and tested using the same dataset.  
 377 This network has approximately 10,000 parameters. Its input signal is a windowed 512 points  
 378 short-time Fourier transform (STFT), split using a Mel-Spectrum front-end. It is processed by 3  
 379 depth-wise convolution layers of 64 features. Complexity of this CNN illustrates how it can be  
 380 difficult to detect cetacean clicks : its corresponding area under the curve (AUC) is 92% for a power  
 381 consumption of 543.51 mW. As shown in Tab.3, proposed ultra-low power detector has an AUC of  
 382 85% (7% less accurate than the CNN solution), but its power consumption is approximately 18000  
 383 times lower. Thus, this makes it particularly relevant to be embedded in a buoy for real time long term  
 384 cetacean monitoring.

	Power Consumption [ $\mu$ W]	AUC [%]
<b>Proposed smart detector</b>	30	<b>85</b>
CNN detector [43]	$54 \times 10^4$	92

**Table 3.** Area Under the Curve (AUC) and power consumption comparison with the state-of-the-art detectors using the labelled database composed of samples from the BOMBYX project sonobuoy [34].

#### 385 4. Conclusion

386 In this paper, a mixed analog-digital always-on ultra-low power smart wake-up based on pulse  
 387 pattern analysis is presented. It is used for triggering a high-performance multi-channel recorder only  
 388 when necessary. Its architecture makes the most of ultra-low power analogical primitives coupled with  
 389 an embedded digital low-power system for fine tuning the pulse detector in order to reduce energy  
 390 consumption. An ultra-low power application to sperm-whales click detection is proposed. Overall

391 measured power consumption of the basic click detector is  $12.5 \mu\text{A}$ . Tested on a labelled dataset that is  
392 more difficult than real conditions, its area under the receiver operating characteristic (ROC) curve is  
393 equal to 75%. It can be improved using expert rules implemented with state machines, leading to an  
394 area under the curve of 85%, while consuming only  $17 \mu\text{A}$  in operational conditions. This allows an  
395 autonomy of 2 years on a single CR2032 battery cell.

396  
397 Further work will focus on more complex pattern analyses, based on same principle : merging  
398 frequency filter bank and heterogeneous temporal features analysis. More precisely, IPI feature for this  
399 species is also being integrated in an enhanced multiscaled version of the state machine to increase  
400 its AUC. Existing CNN is integrating this IPI pattern. One could reach the CNN AUC with this  
401 completed state machine, but in Ultra Low Power. IPI is also an efficient feature to discriminate  
402 between individuals of different sizes, and then to better estimate the number of individuals in an area.  
403 This would be another output of the state machine.

404  
405 CC26

## 406 Acknowledgment

407 The authors thank [Pôle Information, Numérique, Prévention, Santé \(INPS\)](#) of Toulon University  
408 and the Embedded Electronics Technology Platform of Toulon University [Scientific Microsystems for](#)  
409 [Internet of Things \(SMIoT\)](#) [33] for their support in the achievement of this work. They also thank M.  
410 Poupard for labeling sperm whales database. We thank the Scaled Acoustic BIODiversity program  
411 [SABIOD.org](#). This work is partly granted by Chair ADvanced Submarine Intelligent Listening (ADSIL)  
412 ANR-20-CHIA-0014 (<http://bioacoustics.lis-lab.fr>) by Agence National de la Recherche (ANR) 2020-24,  
413 ANR-18-CE40-0014 SMILES, and GIAS (Géolocalisation par Intelligence Artificielle pour la Sécurité  
414 Martime) Intereg Marittimo European whale anti-collision project.

## 415 References

- 416
- 417 1. Glotin, H.; Ricard, J.; Balestrieri, R. Fast Chirplet Transform to Enhance CNN Machine Listening-Validation  
418 on Animal calls and Speech. *arXiv preprint arXiv:1611.08749* **2016**.
  - 419 2. Goëau, H.; Glotin, H.; Vellinga, W.P.; Planqué, R.; Joly, A. LifeCLEF Bird Identification Task 2016: The  
420 arrival of Deep learning. CLEF: Conference and Labs of the Evaluation Forum, 2016, number 1609, pp.  
421 440–449.
  - 422 3. Kobayashi, H.H.; Kudo, H.; Glotin, H.; Roger, V.; Poupard, M.; Shimotoku, D.; Fujiwara, A.; Nakamura, K.;  
423 Saito, K.; Sezaki, K. A Real-Time Streaming and Detection System for Bio-acoustic Ecological Studies after  
424 the Fukushima Accident. In *Multimedia Tools and Applications for Environmental & Biodiversity Informatics*;  
425 Springer, 2018; pp. 53–66.
  - 426 4. Weilgart, L. The impacts of anthropogenic ocean noise on cetaceans and implications for management.  
427 *Canadian Journal of Zoology* **2007**, *85*, 1091–1116, [<https://doi.org/10.1139/Z07-101>]. doi:10.1139/Z07-101.
  - 428 5. Panigada, S.; Pesante, G.; Zanardelli, M.; Capoulade, F.; Gannier, A.; Weinrich, M.T. Mediterranean fin  
429 whales at risk from fatal ship strikes. *Marine Pollution Bulletin* **2006**, *52*, 1287–1298.
  - 430 6. Pennino, M.; Pérez Roda, M.; Pierce, G.; Rotta, A. Effects of vessel traffic on relative abundance  
431 and behaviour of cetaceans: the case of the bottlenose dolphins in the Archipelago de La Maddalena,  
432 north-western Mediterranean sea. *Hydrobiologia* **2016**, *776*, 1–12. doi:10.1007/s10750-016-2756-0.
  - 433 7. Weilgart, L.; Whitehead, H. Group-Specific Dialects and Geographical Variation in Coda Repertoire in  
434 South Pacific Sperm Whales. *Behavioral Ecology and Sociobiology* **1997**, *40*, 277–285.
  - 435 8. Giard, S.; Simard, Y.; Roy, N. Decadal passive acoustics time series of St. Lawrence estuary beluga. *The*  
436 *Journal of the Acoustical Society of America* **2020**, *147*, 1874–1884. doi:10.1121/10.0000922.

- 437 9. Simard, Y.; Roy, N. Detection and localization of blue and fin whales from large-aperture autonomous  
438 hydrophone arrays: A case study from the St. Lawrence estuary. *Canadian Acoustics - Acoustique Canadienne*  
439 **2008**, *36*.
- 440 10. Patris, J.; Malige, F.; Glotin, H.; Asch, M.; Buchan, S.J. A standardized method of classifying pulsed sounds  
441 and its application to pulse rate measurement of blue whale southeast Pacific song units. *The Journal of the*  
442 *Acoustical Society of America* **2019**, *146*, 2145–2154.
- 443 11. Malige, F.; Patris, J.; Buchan, S.J.; Stafford, K.M.; Shabangu, F.; Findlay, K.; Hucke-Gaete, R.; Neira, S.; Clark,  
444 C.W.; Glotin, H. Inter-annual decrease in pulse rate and peak frequency of Southeast Pacific blue whale  
445 song types. *Scientific Reports* **2020**, *10*, 1–11.
- 446 12. Madsen, P.T.; Payne, R.; Kristiansen, N.U.; Wahlberg, M.; Kerr, I.; Møhl, B. Sperm whale sound production  
447 studied with ultrasound time/depth-recording tags. *Journal of Experimental Biology* **2002**, *205*, 1899–1906,  
448 [<https://jeb.biologists.org/content/205/13/1899.full.pdf>].
- 449 13. Møhl, B.; Wahlberg, M.; Madsen, P.; Miller, L.; Surlykke, A. Sperm whale clicks: Directionality and source  
450 level revisited. *The Journal of the Acoustical Society of America* **2000**, *107*, 638–48. doi:10.1121/1.428329.
- 451 14. Giraudet, P.; Glotin, H. Real-time 3D tracking of whales by echo-robust precise TDOA estimates with a  
452 widely-spaced hydrophone array. *Applied Acoustics* **2006**, *67*, 1106–1117.
- 453 15. Glotin, H.; Caudal, F.; Giraudet, P. Whales cocktail party: a real-time tracking of multiple whales.  
454 *International Journal Canadian Acoustics* **2008**, *36*, 7p.
- 455 16. Ferrari, M.; Glotin, H.; Marxer, R.; Asch, M. DOCC10: Open access dataset of marine mammal transient  
456 studies and end-to-end CNN classification. Proc. Int. J. Conf on Neural Net.IJCNN, 2020.
- 457 17. Poupard, M.; Ferrari, M.; Schluter, J.; Marxer, R.; Giraudet, P.; Barchasz, V.; Gies, V.; Pavan, G.; Glotin, H.  
458 Real-time Passive Acoustic 3D Tracking of Deep Diving Cetacean by Small Non-uniform Mobile Surface  
459 Antenna. IEEE International Conference on Acoustics, Speech and Signal Processing (ICASSP), 2019, pp.  
460 8251–8255.
- 461 18. Barchasz, V.; Gies, V.; Marzetti, S.; Glotin, H. A novel low-power high speed accurate and precise DAQ  
462 with embedded artificial intelligence for long term biodiversity survey. In *Proc. of the Acustica Symposium*  
463 **2020**.
- 464 19. Glotin, H.; Thellier, N.; Best, P.; Poupard, M.; Ferrari, M.; Viera, S.; Giés, V.; Oger, M.; Giraudet, P.; Mercier,  
465 M.; Donzé, G.; Campana, M.; Chevallier, J.; Malige, F.; Patris, J.; Prévot, J.; Cosentino, P.; Prévot d’Alvise,  
466 N.; Ourmières, Y.; Barchasz, V.; Lahir, A.; Marzetti, S.; Sarano, F.; Benveniste, J.; Gaillard, S.; de Varenne,  
467 F. *Sphyrna-Odyssée 2019-2020, Rapport I: Découvertes Ethoacoustiques de Chasses Collaboratives de Cachalots*  
468 *en Abysses et Impacts en Mer du Confinement COVID19*; 197p, CNRS LIS, Université de Toulon, 2020. <http://sabiod.org/pub/SO1.pdf>.
- 469
- 470 20. Antao, U.; Choma, J.; Dibazar, A.; Berger, T. 40nW subthreshold event detector chip for seismic sensors.  
471 2015 IEEE International Symposium on Technologies for Homeland Security (HST), 2015, pp. 1–6.  
472 doi:10.1109/THS.2015.7225288.
- 473 21. Jeong, S.; Chen, Y.; Jang, T.; Tsai, J.M.; Blaauw, D.; Kim, H.; Sylvester, D. Always-On 12-nW Acoustic  
474 Sensing and Object Recognition Microsystem for Unattended Ground Sensor Nodes. *IEEE Journal of*  
475 *Solid-State Circuits* **2018**, *53*, 261–274. doi:10.1109/JSSC.2017.2728787.
- 476 22. Abdalla, H.; Horiuchi, T.K. An analog VLSI low-power envelope periodicity detector. *IEEE Transactions on*  
477 *Circuits and Systems I: Regular Papers* **2005**, *52*, 1709–1720. doi:10.1109/TCSI.2005.852203.
- 478 23. Badami, K.M.H.; Lauwereins, S.; Meert, W.; Verhelst, M. A 90 nm CMOS, 6 W Power-Proportional  
479 Acoustic Sensing Frontend for Voice Activity Detection. *IEEE Journal of Solid-State Circuits* **2016**, *51*, 291–302.  
480 doi:10.1109/JSSC.2015.2487276.
- 481 24. Fuketa, H.; O’uchi, S.; Matsukawa, T. A 0.3V 1- $\mu$ W Super-Regenerative Ultrasound Wake-Up Receiver  
482 With Power Scalability. *IEEE Transactions on Circuits and Systems II: Express Briefs* **2017**, *64*, 1027–1031.  
483 doi:10.1109/TCSII.2016.2621772.
- 484 25. Rekhi, A.S.; Arbabian, A. Ultrasonic Wake-Up With Precharged Transducers. *IEEE Journal of Solid-State*  
485 *Circuits* **2019**, *54*, 1475–1486. doi:10.1109/JSSC.2019.2892617.
- 486 26. Fourniol, M.; Gies, V.; Barchasz, V.; Kussener, E.; Barthelemy, H.; Vauché, R.; Glotin, H.  
487 Analog Ultra Low-Power Acoustic Wake-Up System Based on Frequency Detection. 2018 IEEE  
488 International Conference on Internet of Things and Intelligence System (IOTAIS), 2018, pp. 109–115.  
489 doi:10.1109/IOTAIS.2018.8600849.

- 490 27. Woias, P.; Heller, S.; Pelz, U. A highly sensitive and ultra-low-power wake-up receiver for  
491 energy-autonomous embedded systems. *Journal of Physics: Conference Series* **2018**, *1052*, 012024.  
492 doi:10.1088/1742-6596/1052/1/012024.
- 493 28. Pletcher, N.M.; Gambini, S.; Rabaey, J.M. A 2GHz 52 uW Wake-Up Receiver with -72dBm Sensitivity Using  
494 Uncertain-IF Architecture. 2008 IEEE International Solid-State Circuits Conference, Digest of Technical  
495 Papers, 2008, pp. 524–633.
- 496 29. Fourniol, M.; Gies, V.; Barchasz, V.; Kussener, E.; Barthelemy, H.; Vauché, R.; Glotin, H. Low-Power  
497 Wake-Up System based on Frequency Analysis for Environmental Internet of Things. 2018 14th  
498 IEEE/ASME International Conference on Mechatronic and Embedded Systems and Applications (MESA),  
499 2018, pp. 1–6.
- 500 30. Xiaoqiong Zuo.; Liu Yaxian. Low power performance achievement in embedded system. 2011  
501 2nd International Conference on Artificial Intelligence, Management Science and Electronic Commerce  
502 (AIMSEC), 2011, pp. 4655–4658.
- 503 31. Magno, M.; Cavigelli, L.; Mayer, P.; v. Hagen, F.; Benini, L. FANNCortexM: An Open Source Toolkit for  
504 Deployment of Multi-layer Neural Networks on ARM Cortex-M Family Microcontrollers : Performance  
505 Analysis with Stress Detection. 2019 IEEE 5th World Forum on Internet of Things (WF-IoT), 2019, pp.  
506 793–798.
- 507 32. Marzetti, S.; Gies, V.; Barchasz, V.; Barthélemy, H.; Glotin, H.; Kussener, E.; Vauché, R. Embedded Learning  
508 for Smart Functional Electrical Stimulation. 2020 IEEE International Instrumentation and Measurement  
509 Technology Conference, 2020.
- 510 33. Gies, V.; Barchasz, V.; Glotin, H. SMIOT: Scientific Microsystems for the Internet of Things, Technological  
511 Platform. <http://www.smiot.fr>.
- 512 34. Glotin, H.; Giraudet, P.; Ricard, J.; Malige, F.; Patris, P.; Roger, V.; Prévot, J.M.; Poupard, M.; Philippe, O.;  
513 Cosentino, P. Projet VAMOS : Visées aériennes de mammifères marins jointes aux observations acoustiques  
514 sous-marines de la bouée BOMBYX et Antares: nouveaux modèles en suivis et lois allométriques du  
515 *Physeter macrocephalus*, *Ziphius Cavirostris* et autres cétacés. Technical report, Univ. Toulon, 2017. [http://sabiody.org/pub/PELAGOS\\_VAMOS.pdf](http://sabiody.org/pub/PELAGOS_VAMOS.pdf).
- 516
- 517 35. Maxim. MAX409 : 1.2 uA Max, Single/Dual/Quad, Single-Supply Op Amps. Rev. 4.
- 518 36. Diodes Incorporated. SD103AW : Schottky barrier diode. Rev. 25.
- 519 37. Texas Instruments. LPV811 : Precision 425 nA nanopower operational amplifiers. Rev. 2016.
- 520 38. Analog Devices. AD5222 : Increment/Decrement Dual Digital Potentiometer. Rev. 0.
- 521 39. Texas Instruments. CC2652R : SimpleLink™ Multiprotocol 2.4 GHz Wireless MCU, 2018. Rev. 04/2020.
- 522 40. Linear Technology. LTC1662 : Ultralow Power, Dual 10-Bit DAC in MSOP. Rev. A.
- 523 41. Texas Instruments. MCP1810 : Ultra-Low Quiescent Current LDO Regulator, 2016. Rev. 2018.
- 524 42. ST. TS881 : Rail-to-rail 0.9 V nanopower comparator. Rev. 2.
- 525 43. Best, P.; Marzetti, S.; Poupard, M.; Ferrari, M.; Paris, S.; Marxer, R.; Philippe, O.; Gies, V.; Barchasz, V.;  
526 Glotin, H. Stereo to five-channels bombyx sonobuoys from four years cetacean monitoring to real-time  
527 whale-ship anti-collision system. *In Proc. of the Acustica Symposium* **2020**.